

# Dual Effect of Light Irradiation for Surface Relief Gratings Formation in Se-rich Ge-Se Thin Films

Tyler Nichol<sup>1</sup>, Janis Teteris<sup>2</sup>, Mara Reinfelds<sup>2</sup>, Maria Mitkova<sup>1,\*</sup>

<sup>1</sup>Department of Electrical and Computer Engineering, Boise State University, Boise, ID 83725-2075, USA

<sup>2</sup>Institute of Solid State Physics, University of Latvia, Riga, Latvia

\*Corresponding author: E-mail: mariamitkova@boisestate.edu

Received: 28 February 2019, Revised: 11 March 2019 and Accepted: 30 April 2019

DOI: 10.5185/amlett.2019.0012

www.vbripress.com/aml

## Abstract

Relief surface formation as a result of light irradiation is one important property of chalcogenide glasses which gives rise of number of applications. Understanding the nature of the process is an essential step towards optimization of the relief images obtained. This work depicts the mechanisms for surface relief grating formation in Ge-Se thin films exposed to diffracted light. A dependence on the period of the illumination source is revealed, which correlates with the composition of the thin film material. Raman spectroscopy, Energy Dispersive Spectroscopy (EDS), and Atomic Force Microscopy (AFM) were used to analyze the films. The results point towards a dual effect of light irradiation leading to mass transport and structural changes, which results in a surface relief formation. Copyright © VBRI Press.

**Keywords:** Chalcogenide glass, thin film, surface relief grating, diffraction, mass transport.

## Introduction

The photoinduced effects in chalcogenide glasses engage the interest of scientists and engineers for more than half a century, and this field still offers great opportunities for research to give answers to unresolved problems. The underlying fundamental understanding of these phenomena poses challenges and excites the experimentalist and theorist to look for solutions – as noted in number of review articles [1]. The photoinduced effects arise from the transformations that occur in glass structure after its electrons are excited by the light [2]. These effects manifest themselves in many different ways, engaging changes not only in the optical performance but also in thermal properties, structure and others [3-6]. The reasons for the occurrence of this plurality of radiation induced phenomena are mainly the electronic and atomic structure, and lack of periodicity of the structural organization in chalcogenide glasses [7-9]. They are semiconductors with an energy gap of 1-3 eV. However, a unique feature is the availability of states in the band gap due to the lack of long range order and the presence of lone pair electrons located at the chalcogen atoms [7]. This triggers excitation effects by the interaction of the chalcogenide glasses with a wide range of wavelengths, leading to different structural effects [10-13]. Furthermore, excited carriers are effectively localized in disordered and defective glass structures, and they undergo strong electron-lattice interactions which have been modeled [14, 15].

One very important effect that has drawn special attention is the fact that the chalcogenide glasses change their volume upon irradiation with light, and undergo either photocontraction or photoexpansion depending upon the glass composition and the radiation conditions [16-20]. The volume expansion profile reproduces the transversal distribution of the intensity of the inducing single beam or of the spatial patterns of two interfering beams. Consequently, microlenses [21] or profile gratings [22] can be fabricated on the surface of the sample without any intermediate steps.

The photoinduced thickness changes in amorphous Se/As<sub>2</sub>S<sub>3</sub> and similar multilayers have been studied [23]. A. Saliminia *et al.* [24] have proposed that the process of mass transport takes place due to electric field gradient force of the excitation light. The resulting volume changes in the material could be related to the nonradiative relaxations of the photoexcited carriers, which may create additional anisotropic molecular units in chalcogenide glasses, for example oppositely charged chalcogen pairs, defects etc. [25], which are in principle long-living. During illumination, light is exponentially attenuated in depth inside the film and this produces a non-uniform refractive index profile. An immediate consequence of this attenuation of the refractive index profile is that the effective thickness of the irradiated film is determined by the penetration depth of the polarized light. This effective thickness does not depend

on the physical thickness, but on the chemical composition of the film and light wavelength used. There are two competing processes involved – on one hand the light must be effectively absorbed by the film to decrease the exposure dose; on the other hand, the light must penetrate into the film deep enough to provide for the conditions of obtaining a high value of diffraction efficiency.

The basic understanding is that the volume changes and related relief formation in chalcogenide glasses can effectively be associated to occurrence of some sort of mass transport in them. It is related to the fact that the band-gap photoexcitation and relaxation of carriers in these materials create anisotropic molecular units and defects with higher dielectric polarizabilities. In addition, significant photoinduced softening of the matrix is achieved due to the bond cleavage and stress relaxation [26]. Then, a photoinduced drift of units in the non-uniform electric field of light takes place, which leads to a mass transport and formation of giant relief modulations mostly used for formation of relief diffraction gratings [27]. However, a question occurs: is the mass transport the only reason for the relief formation? Furthermore, it has never been studied what exactly moves – the entire matrix of the glass, or some specific structural units and if there is a compositional and structural difference in the material of the peaks and valleys of the newly formed relief structures.

In this work thin films of Se-rich Ge-Se glasses have been investigated using AFM, EDS, and Raman spectroscopy in order to clarify details of the effects occurring at relief diffraction gratings formation through coherent multiple-beam interference illumination. These materials have high structural flexibility and thus impose formation of relief with well-expressed minima and maxima. With this study we give answer of the questions if the relief is result of mass transport only, what structural units are participating in the mass transport during the relief formation and if there are structural and compositional changes occurring at this process.

## Experimental

Bulk Chalcogenide glasses with composition  $\text{Ge}_{10}\text{Se}_{90}$  and  $\text{Ge}_{15}\text{Se}_{85}$  were prepared from high purity germanium and selenium by using the traditional melt – quench technique. Thin films of these glasses were deposited on Si substrates using a Cressington 308R evaporation system at a pressure of  $1 \times 10^{-6}$  mbar, non-controlled substrate temperature, from a semi-Knudsen cell for preserving the source composition in the thin films. The film thickness was 2  $\mu\text{m}$ , and the deposition process occurred at room temperature. No annealing was performed before holographic recordings were created.

The surface relief grating (SRG) formation over the thin chalcogenide glass films was achieved by two-beam traditional [27] symmetric holographic transmission

scheme. Recording of SRG was performed by Cobolt laser  $\lambda = 594$  nm wave-light beams of equal intensities  $I_1 = I_2 = 0.3$  W/cm<sup>2</sup>; grating periods was changed from  $\Lambda \approx 1$   $\mu\text{m}$  to  $\approx 11$   $\mu\text{m}$ . The orthogonally  $\pm 45^\circ$  linearly and right or left circularly polarised light beams were used for recording thus providing the optimal conditions for surface relief grating formation [28-30]. It should be noted that in this case SRG recording is determinate by the modulation of light electric field (for such polarisation configuration of recording beams, light intensity distribution is practically uniform). The surface relief structure was studied under an Atom Force Microscope (AFM) after recording of SRG with exposure dose  $E \approx 10.8$  kJ/cm<sup>2</sup> for all studied cases.

The corrugated surface relief (CSR) structure formed after irradiation of the films was studied using OTESPA probe on a Veeco Dimensions 3100 Atom Force Microscopy (AFM) system equipped with Nanoscope IV controller in tapping mode.

Energy Dispersion Spectroscopy (EDS), used to confirm the exact composition of the produced films, as well as the composition of the peaks and valleys of the created relief, was conducted using an Hitachi S-3400N II Scanning Electron Microscope (SEM) with an Oxford Instruments Energy + EDS system at a working distance of 10 nm and x 2,000 magnification with 90s collection time. Each sample was measured at five different locations for the collection of an accurate average and the standard deviation.

The structure of the films was studied by micro-Raman spectroscopy using an Horiba Jobin Yvon T64000 triple monochromator with a liquid-nitrogen-cooled multichannel charge-coupled devices detector and He-Ne laser source, emitting at 633 nm. The system had a microscope which allowed exact positioning of the laser beam for measuring the structure of the peaks and valleys of the created relief.

## Results

**Fig. 1 (a-c)** show the AFM results from measuring of the surface profile of gratings written on  $\text{Ge}_{15}\text{Se}_{85}$  with different periods. As evidenced from these figures for  $\text{Ge}_{15}\text{Se}_{85}$  decreasing the period leads to decrease in the relief height, and an increase of the surface roughness. In addition to this, the relief structure becomes less sinusoidal as the diffraction grating period is decreased.

**Figs. 1 (d-f)** show the AFM results of  $\text{Ge}_{10}\text{Se}_{90}$ , which have similar results as the previous composition, with key differences at smaller diffraction period.  $\text{Ge}_{10}\text{Se}_{90}$  films are more sensitive towards relief formation. There is an exclusion related to the relief with the biggest period, which we will discuss later in this work. Notably, the sinusoidal pattern of the relief does not break down as the period is decreased, and this film composition is more responsive to grating formation at lower periods, compared to  $\text{Ge}_{15}\text{Se}_{85}$ .

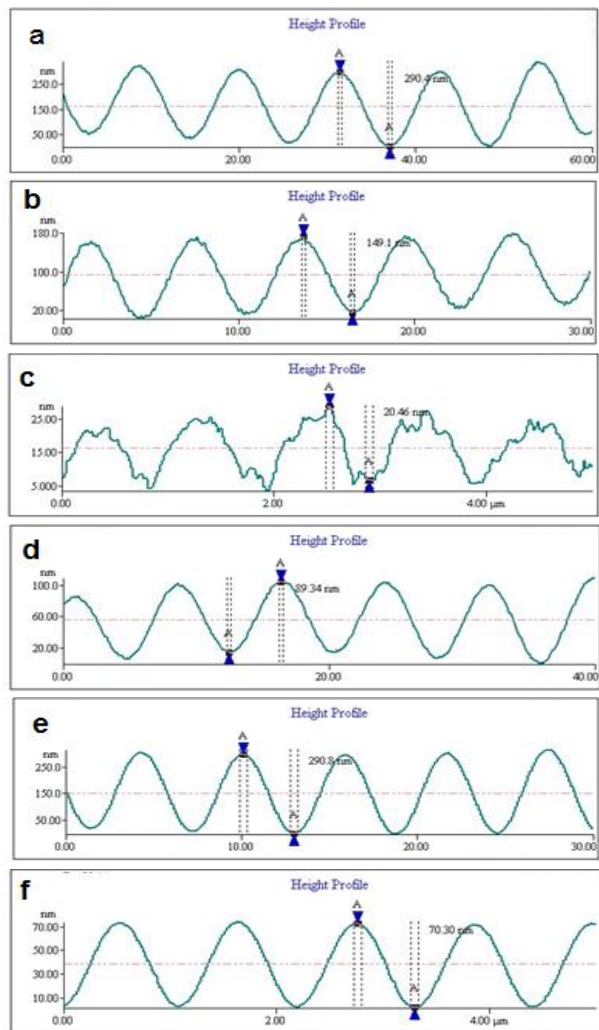


**Fig. 1.** AFM Measurement of Surface Profile of Ge-Se films Following Irradiation by 594 nm Laser: (a)  $Ge_{15}Se_{85}$  film, 11.4  $\mu m$  Period; (b)  $Ge_{15}Se_{85}$  film, 5  $\mu m$  Period; (c)  $Ge_{15}Se_{85}$  film, 1  $\mu m$  Period; (d)  $Ge_{10}Se_{90}$  film, 7.8  $\mu m$  Period; (e)  $Ge_{10}Se_{90}$  film, 5.8  $\mu m$  Period; (f)  $Ge_{10}Se_{90}$  film, 1  $\mu m$  Period.

**Fig. 2** displays an SEM micrograph of the irradiated area. The contrast between the high and low parts seen in the micrograph can be attributed to the geometry of the detector and the probe electron beam. The material itself does not have enough Z-contrast to create the distinction between these areas, but because of the angle between the sample and the detector, the relief pattern shadows some of the secondary emitted electrons, allowing accurate placement of the electron beam for the measurements.

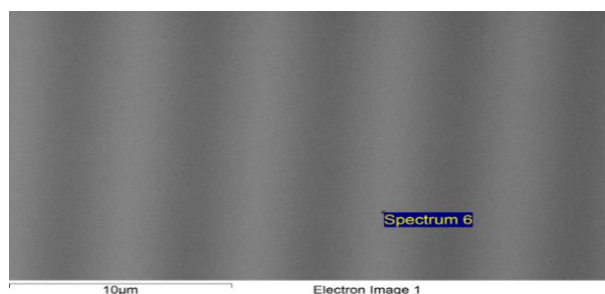


**Fig. 2.** SEM Micrograph of SRG in  $Ge_{15}Se_{85}$ .

Measurements were taken in five areas and averaged in each part of the sample in nominal compositions of  $Ge_{10}Se_{90}$ , and  $Ge_{15}Se_{85}$ , which refer to the composition of the bulk material from which they were made. The results of composition measurements can be seen in **Table 1**.

**Table 1.** Results of EDS Measurements Taken of Surface Relief Gratings.

Virgin Composition	Top of SRG	Bottom of SRG
$Ge_{19.1}Se_{80.9}$	$Ge_{18.7}Se_{81.3}$	$Ge_{19.6}Se_{80.4}$
$Ge_{24.2}Se_{75.8}$	$Ge_{23.7}Se_{76.3}$	$Ge_{24.7}Se_{75.3}$

**Figs. 3 (a - c)** display fitting of the Raman data of measurements to the high and low parts of the SRG.

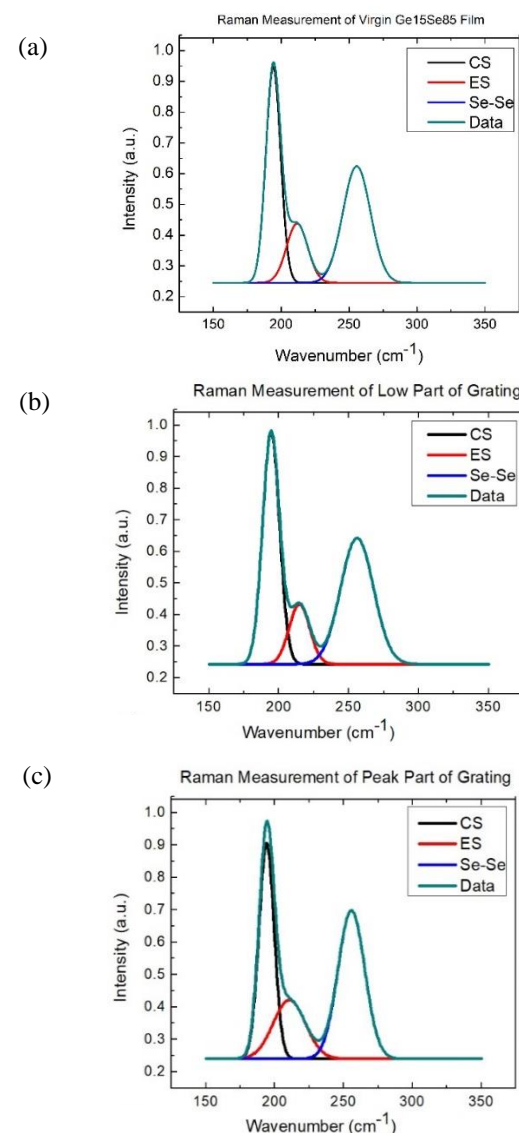


**Fig. 3.** Raman Fitting of SRG on  $Ge_{15}Se_{85}$  (a) from virgin samples (b) from the low and (c) from the peak sections.

Raman measurements indicate that irradiation causes changes to the thin films' structure, which varies with the high and low parts of the SRG. The plot in **Fig. 3 (b)** displays the same peak signatures found in

**Table 2.** Analysis of Raman Peaks from Measurements of SRG.

Associated Structural Unit	Peak Center Virgin	Peak Center (High)	Peak Center (Low)	Areal Intensity Virgin	Areal Intensity (High)	Areal Intensity (Low)
CS	194 cm <sup>-1</sup>	194 cm <sup>-1</sup>	194 cm <sup>-1</sup>	39.73%	43.16%	35.66%
ES	211 cm <sup>-1</sup>	215 cm <sup>-1</sup>	211 cm <sup>-1</sup>	15.82%	13.24%	19.68%
Se-Se	256 cm <sup>-1</sup>	256 cm <sup>-1</sup>	256 cm <sup>-1</sup>	44.02%	44.66%	43.6%

**Fig. 3 (a)**, but the areas under each of these peaks are slightly different as a result of irradiation. The peak associated with edge-sharing (ES) structures has broadened slightly and shifted from 211 cm<sup>-1</sup> to 215 cm<sup>-1</sup> in the top of the SRG. **Table 2** provides information on the peak locations and areal intensity of each peak.

## Discussion

There are several aspects of the processes and results which need to be well understood and interpreted. In essence, there is no doubt in the research community dealing with studies of surface relief gratings that both the light intensity and the electric field carried by light variations are essential for their formation [31].

A number of proposed models for explaining the origin of the driving forces responsible for surface relief gratings formation under the light illumination on the molecular level, including mean-field theory [32], permittivity gradient theory [33], gradient electric force model [34], are based on electromagnetic forces of the excitation light. The spatial variation of the light (both intensity and polarization) leads to a variation of the material electrical susceptibility. The electric field of the incident light then leads to a polarization of the material. Forces are expected to occur between a polarized material and a light field gradient in a similar way as a dipole experiencing an electric field gradient. The question arises as to how the recording media components are affected by light illumination.

Surface relief gratings of period  $\Lambda = 33\mu\text{m}$  were recorded in As-S-Se film and scanning electron microscopy (SEM) microanalysis of chemical composition of grating relief top and bottom places was performed [22]. Periodic oppositely directed concentration changes of As and Se related to grating period were observed. However, chalcogenide glasses are very sensitive towards electron beam irradiation which makes the validity of the obtained results questionable, i.e. it is not clear if they are result of the light irradiation and relief formation or of the electron beam irradiation. According to [35] the presence of polar As<sub>4</sub>S<sub>3</sub> molecules, which are sensitive to the electric field generated by the laser, is responsible for observed laser-induced mass transport effect in amorphous As-S films.

Because of the periodicity of the light modulation, the formed surface relief has a sinusoidal character, which is preserved at all periodic structures except the

smallest period of 1  $\mu\text{m}$  for the Ge<sub>15</sub>Se<sub>85</sub> films. We suggest that some interference of the electric field distribution occurs due to the high frequency of the film polarity change, which causes deformations in the occurring relief. It is not visible in the case of Se richer samples, such as Ge<sub>10</sub>Se<sub>90</sub>, because of the higher concentration of the flexible element (Se), which is quite mobile and distributes well, resulting in sinusoidal relief formation even at the smallest period attempted. This is also evidenced by measurements of photoinduced birefringence [31], which indicates an increase in the value of birefringence and a decrease in induction time with an increase in Se concentration.

The growth of the surface relief gratings becomes saturated at long inscription times (please recall that in our experiments recording exposure dose is of 10.8 kJ/cm<sup>2</sup>). There is a difference between saturation values of surface relief gratings' depth ( $\Delta h_{\text{sat}}$ ) in Ge<sub>10</sub>Se<sub>90</sub> and Ge<sub>15</sub>Se<sub>85</sub> films with comparable periods. The greater changes are observed in the Ge<sub>10</sub>Se<sub>90</sub> films (see **Fig. 1 a - f**). According to [36] at large deformations the force of surface tension becomes comparable to the inscription force and therefore plays an essential role in the retardation of the inscription process. It is equal to zero when the surface is flat and increases proportionally to the surface relief depth. The process of saturation depends upon the counterbalance between the inscription force and the force of surface tension. This balance can be shifted in favor of the inscription force by a decrease of surface tension of recording medium. Melnichenko *et al.* [37] report that the values of surface tension for Ge<sub>10</sub>Se<sub>90</sub> and Ge<sub>15</sub>Se<sub>85</sub> are 0.136 J/m<sup>2</sup> and 0.158 J/m<sup>2</sup>, respectively. The glass transition temperature of the recording material can also affect the relief formation efficiency.  $T_g$  for Ge<sub>10</sub>Se<sub>90</sub> and Ge<sub>15</sub>Se<sub>85</sub> are 377 K and 413 K [36], respectively.

From the EDS data it is visible that the real composition of the virgin films is different than that of the bulk material from which the films have been deposited. For clarity of the text we used the data related to the bulk material, but in essence the films were richer in Ge than the source material. The reason for this is that Se has much higher partial pressure than Ge. It evaporates faster and in fact reaches the substrate with much higher energy than Ge at a constant temperature, which causes repulsion of part of the atoms that impinge on the substrate. Due to the higher kinetic energy of Se atoms, travelling towards the substrate, more of the evaporated atoms from the bulk material are reflected

from the substrate, compared to Ge atoms, which reach the substrate, resulting in reduced Se concentration in the thin films compared to the source material. This known phenomenon is one of the limitations of physical vapor deposition, especially when working with materials containing elements of varying partial pressures.

The EDS data give further very important information about the composition of the tops and the bottoms of the formed relief structure resulting in Se richer tops and Ge richer bottoms. This is one indication that Se is the more mobile element in the films not only because of its higher partial pressure, which should move it during the heating accompanying the relief formation, but also because of the lower coordination of this element. Obviously, it is much easier to break the two covalent bonds connecting Se to other Se/Ge atoms, or include it in tetrahedral structural units, than to liberate Ge, which has tetrahedral coordination. So we consent with the idea that the relief is due to a material heating and mass transport [38] with the remark that not all material components of the film move as a whole, but there are more, and less mobile atoms – in the studied case, mobile Se and less mobile Ge. This leads to some compositional differences between the material in the top and the bottom of the formed relief and is expected to cause structural changes in the material.

Proof of the structural changes occurring during the relief formation has been evident by the Raman spectroscopy studies. In essence, the Raman spectra indicate the film's structural characteristics and correlate them with the compositional data of the films. The spectra demonstrate the presence of corner-sharing (CS) tetrahedral structural units at  $194\text{ cm}^{-1}$  edge-sharing (ES) at  $211\text{ cm}^{-1}$  ( $215\text{ cm}^{-1}$  for the peaks in the relief structures) and Se-Se chains at  $256\text{ cm}^{-1}$ . This data coincide well with the structural characteristics for Ge-Se glasses reported by S. Bhosle *et al.* [39] The shift in the ES Raman mode frequency would resemble formation of structure with lower Se content [40]. The appearance of the ES structural units is related to the big difference of their population in the valleys and the peaks of the structure, which looks like material with quite different composition. As shown in **Table 1** there is not a high compositional difference, but there is a significant increase of the population of the CS structural units, and decrease of the ES structural units due to their transformation - ES to CS structures and opening of the structure [41] in the peaks of the relief. This structure has much lower density, and its appearance, along with mass transport, is the second major reason for increase of the peaks' height. There is an interesting interplay in the peaks formed structure, which shows better organization in the ES part where the peak becomes sharper in the valley parts which reduces their volume, and in the same time increased lack of organization in the Se chains. In essence, the effects occurring among the Se chains have a leading role in the relief formation. Looking at the percentage appearance of different structural units, there is an interesting fact – the areal intensity of the CS in the peaks is 7.5% higher than in the valleys. At the same

time, the decrease of the % appearance of the ES structure and increase of the % amount of the Se-Se chains together is also 7.5%. This indicates that the free moving Se atoms do not become members of the tetrahedral structures, but remain in chain units, and the volume increase in the peaks is mainly caused by the interplay of the tetrahedral structural units and particularly the transition of some ES structural units to CS structural units. This is initiated by the charge distribution, which is denser and leads to structural polarization in the ES structural units, due to the closer proximity of the Se atoms, where the negative charge is concentrated. The interaction of these polarized structures with the light's electrical field is the reason for the appeared structural reorganization.

The experimental result which needs specific explanation is the fact of obtaining of a very low difference in the height of the peaks and valleys for period of  $7.8\text{ }\mu\text{m}$  for  $\text{Ge}_{10}\text{Se}_{90}$ . In essence, this should be the more sensitive material because of the higher concentration of Se and this is the case for the measurements related to the  $5\text{ }\mu\text{m}$  and  $1\text{ }\mu\text{m}$  periods. As is known, the Se rich glasses are particularly inhomogeneous because of the high concentration of Se chains [42]. It is for this reason that there is also some lack of consistency in the results. The experimental data have been collected from several different positions in the films, but the average result is the one presented in **Table 1**. Consequently the lack of structural homogeneity in the films affected some of the results. There is another important factor in the interaction of Se with the light vector, which creates photo-electronic excitation [43] in its specific structure, combined by one dimensional chains. This structure can be well segmented [44] by which local alignment of the chains can occur resulting in reduction of the structure volume.

## Conclusion

In this study we researched the mechanism of formation of surface relief gratings in thin films of very Se rich Ge-Se glasses. The formation of such gratings is due to reorientation and arrangement of electric field sensitive structural units (dipoles) of recording material by linearly polarized light components of an illumination pattern. These orientated structural units can be displaced by the gradient force of an inhomogeneous electric field created by linearly polarized light components of the interference pattern.

During this process mass transport occurs, along with molecular restructuring, which causes formation of the relief structure. This study shows that large tetrahedral units are moving, forced by the electrical field created by light, but Se is the more mobile part of the structure and moves individually as well. In this manner compositional difference is created within the valleys and the peaks of the formed relief. This composition change affects, to some extent, the overall structure of the material, and is accompanied with transformation of the ES units to CS units in the peaks of

the formed relief, which results in a volume effect with lower density. In this manner we gave an evidence for the dual character of the materials changes for formation of relief structure – as mass transport with predominantly individual movement of the chalcogenide atoms and structural reorganization towards structure with lower density and greater volume in the peaks of the relief structure.

## References

1. Kolobov, A. V.; Editor: Photo-Induced metastability in Amorphous Semiconductors, Wiley-VCH GmbH & Co. KGaA, Weinheim, **2003**.
2. Mitkova, M.; Real time Optical recording on Thin Films of Amorphous Semiconductors, in Insulating and Semiconducting Glasses, P. Boolchand editor, World Scientific, Singapore, New Jersey, London, Hong Kong, **2000**, p. 813-843.
3. Ganjoo, A.; Shimakawa, K.; Kitano, K.; Davis, E. A.; *J. Non-Cryst. Sol.*, **2002**, 299, 917.
4. Chen, G.; Jain, H.; Vlcek, M.; Khalid, S. J. Li; Drabold, D. A.; Elliott, S.R.; *Appl. Phys. Lett.*, **2003**, 82, 706.
5. Ston, R.; Vlcek, M.; Jain, H.; *J. Non-Cryst. Sol.*, **2003**, 326, 220.
6. Jain, H.; Photoinduced Atom Displacement in Solids: Glasses vs. Polymers, in: Physics and Applications of Disordered Materials, M. Popescu editor, INOE Publ., **2002**, 169.
7. Fritzsche, H.; Light Induced Structural Changes in Glasses in Insulating and Semiconducting Glasses, P. Boolchand editor, World Scientific, Singapore, New Jersey, London, Hong Kong, **2000**, p. 653.
8. Neufville, J. P. De; Moss, S. C.; Ovshinsky, S. R.; *J. Non-Cryst. Sol.*, **1974**, 13, 191.
9. Tanaka, K.; *J. Non-Cryst. Sol.*, **1980**, 35, 1023.
10. Spence, C. A.; Elliott, S. R.; *Phys. Rev.*, **1989**, B39, 5452.
11. Yang, C. Y.; Paesler, M. A.; Sayers, D. E.; *Phys. Rev.*, **1987**, B36, 9160.
12. Chen, G.; Jain, H.; Khalid, S.; Li, J.; Drabold, D. A.; Elliott, S. R.; *Solid St. Commun.*, **2001**, 120, 149.
13. Chen, G.; Jain, H.; Vlcek, M. J. Li; Drabold, D. A.; Khalid, S.; Elliott, S. R.; *J. Non-Cryst. Sol.*, **2003**, 326, 257.
14. Lee, J. M.; Paesler, M. A.; Sayers, D. E.; Fontaine, A.; *J. Non-Cryst. Sol.*, **1990**, 123, 295.
15. Drabold, D. A.; Zhang, X. J. Li; First principle molecular dynamics and photostructural response in amorphous silicon and chalcogenide glasses in Photo-induced metastability in amorphous semiconductors, Ed. by A. V. Kolobov, Wiley-VCH, Weinheim, **2003**, p. 260-276.
16. Hisakuni, H.; Tanaka, Ke.; *Appl. Phys. Lett.*, **1994**, 65, 2925.
17. Tanaka, Ke.; *Phys. Rev. B*, **1998**, 57, 5163.
18. Loeffler, P.; Schwartz, T.; Sautter, H.; Lezal, D.; *J. Non-Cryst. Sol.*, **1998**, 232, 526.
19. Poborchii, V. V.; Kolobov, A. V.; Tanaka, Ke.; *Appl. Phys. Lett.*, **1999**, 74, 215.
20. Gump, J.; Finkler, I.; Xia, H.; Sooryakumar, R.; Bresser, W. J.; Boolchand, P.; *Phys. Rev. Lett.*, **2004**, 92, 24550.
21. Hisakuni, H.; Tanaka, Ke.; *Opt. Lett.*, **1995**, 20, 958.
22. Reinfelde, M.; Teteris, J.; *J. Optoelectron. Adv. Mat.*, **2011**, 13, 1531.
23. Ivan, I.; Kikineshi, A.; *J. Optoelectron. Adv. Mat.*, **2002**, 4, 743.
24. Saliminia, A.; Galstian, T.; Villeneuve, A.; *Phys. Rev. Lett.*, **2000**, 85, 4112.
25. Tikhomirov, V. K.; *J. Non-Cryst. Sol.*, **1999**, 256, 328.
26. Tanaka, K.; Shimikawa, K.; *J. Non-Cryst. Sol.*, **2018**, 481, 579.
27. Gertners, U.; Teteris, J.; The impact of light polarization on the direct relief forming processes in As<sub>2</sub>S<sub>3</sub> thin films, IOP Conf. Series: Materials Science and Engineering, 38, 012026, **2012**.
28. Gertners, U.; Teteris, J.; *Opt. Mat.*, **2010**, 32, 807.
29. Asatryan, K.E.; Galstian, T.; Vallee, R.; *Phys. Rev. Lett.*, **2005**, 94, 087401.
30. Gertners, U.; Teteris, J.; *Adv. Mater.*, **2009**, 11, 1963.
31. Reinfelde, M.; Mitkova, M.; Nichol, T.; Ivanova, Z. G.; Teteris, J.; *Chalcogenide Letters*, **2018**, 15, 35.
32. Pederson, T.G.; Johansen, P.M.; Holme, N.C.; Ramanujam, P.S.; *Phys. Rev. Lett.*, **1998**, 80, 89.
33. Yager, K.G.; Barret, C.J.; *Current Opinion Sol. St. Mat. Sc.*, **2001**, 5, 487.
34. Kumar, J.; Li, L.; Jiang, X.; Kim, D.; Lee, T.; Tripathy, S.; *Appl. Phys. Lett.*, **1998**, 72, 2096.
35. Kondrat, O.; Holomb, R.; Csik, A.; Takats, V.; Veres, M.; Mitsa, V.; *Nanoscale Research Lett.*, **2017**, 12, 149.
36. Saphiannikova, M.; Geue, T.M.; Henneberg, O.; Morawetz, K.; Pietsch, U.; *J. Chem. Phys.*, **2004**, 120, 4039.
37. Melnichenko, A.T.; Fedelech, V.; Melnichenko, T.; Sanditov, D.; Badmaev, S.; Damdinov, D.; *Glass Phys. Chem.*, **2009**, 35, 32.
38. Bohdan, R.; Molnar, S.; Csarnovic, I.; Veres, M.; Csik, A.; Kokenyesi, S.; *J. Non-Cryst. Sol.*, **2015**, 408, 57.
39. Bhosle, S.; Gunasekera, K.; Chen, Ping; Boolchand, P.; Micoulaut, M.; Massobrio, C.; *Solid State Communications*, **2011**, 151, 1851.
40. Boolchand, P.; Gunasekera, K.; Bosle, S.; *Phys., Stat. Sol. B.*, **2012**, 249, 1.
41. Edwards, T. G.; Sen, S.; *J. of Phys. Chem. B*, **2011**, 115, 4307.
42. Shatnawi, M. T. M.; Farrow, Ch. L.; Chen, P.; Boolchand, P.; Sartbaeva, A.; Thorpe, M. F.; Billinge, S. J. L.; *Phys. Rev. B*, **2008**, 77, 094134.
43. Tanaka, K.; *J. Non-Cryst. Sol.*, **2018**, 500, 272.
44. Tanaka, K.; Asao, H.; *Jpn. J. Appl. Phys.*, **2006**, 45, 1669.